Synthesis, Properties, and Structural Characterization of Bromo- and Iodotetracarboxylatodiruthenium(II,III) Compounds

M. Carmen Barral,[a] Rodrigo González-Prieto,[a] Reyes Jiménez-Aparicio,*[a] J. Luis Priego,[a] M. Rosario Torres,[b] and Francisco A. Urbanos[a]

Keywords: Carboxylate ligands / Metal-metal interactions / Multiple bonds / Ruthenium / Solvatochromism

The synthesis and characterization of the compounds $[Ru_2X(\mu\text{-}O_2CPh)_4]_n$ [X = Br (**1**), I (**2**)] and $[Ru_2X(\mu\text{-}O_2CC_6H_4\text{-}p\text{-}OMe)_4(H_2O)]$ [X = Br (**3**) and I (**4**)] is described. The structures of these compounds were determined by single-crystal X-ray diffraction. The molecular structures of $[Ru_2Br(\mu\text{-}O_2CCMePh_2)_4(EtOH)\cdot 0.5EtOH]$ (**5**·0.5EtOH) and $[Ru_2I(\mu\text{-}O_2CCMePh_2)_4(MeOH)\cdot 0.5H_2O]$ (**6**·0.5H_2O) are also reported. Complexes **1** and **2** show a zigzag polymeric arrangement with the diruthenium units linked by bromide and iodide ligands, respectively. The molecular nature of compounds **3** and **4** shows the influence of the axial ligand in the arrangement in the solid state, which contrasts with the polymeric structure found in all chlorodiruthenium(II,III) derivatives with arenecarboxylate bridging ligands. The Ru–Ru bond lengths for all complexes range from 2.2756(17) to 2.2906(7) and 2.273(3) to 2.2965(6) Å for the bromide and iodide derivatives, respectively. This study demonstrates that the nature of the axial ligand plays an important role in the arrangement in the solid state and in the electronic properties of the halotetracarboxylatodiruthenium(II,III) complexes. Thus, the iodo derivatives show an intense solvatochromism, whereas the solvatochromism is slight in the bromo derivatives and is not observed in the chloro complexes.

Introduction

The synthesis and properties of the diruthenium(II,III) complexes of formula $[Ru_2Cl(\mu\text{-}O_2CR)_4]$ (R = alkyl, aryl) have attracted much attention, mainly due to the interest in their electronic and magnetic properties.[1−3] The use of these complexes as building blocks in the formation of supramolecular species has increased this interest.[4] Much effort has been devoted to the assembly of dinuclear units and a wide variety of oligomers and polymers have been isolated. These new materials containing diruthenium units may display novel conductive, optical, and magnetic properties.[1−4] In $[Ru_2Cl(\mu\text{-}O_2CR)_4]$ compounds the ruthenium atoms are strongly bonded by four bridging carboxylate ligands, with one axial position occupied by a chloride ion.[1−3] The chloride ligand of the $[Ru_2Cl(\mu\text{-}O_2CR)_4]$ molecule is usually bonded to the free axial position of a neighboring diruthenium unit leading to zigzag or linear chains.[4−15] However, a neutral ligand can also coordinate to the free axial position giving discrete dinuclear molecules.[16−19] Both discrete molecules and polymeric species with 2,2-diphenylpropionate and axial chloride ligands have been reported.[11,19] Thus, the influence of the carboxylate bridging group on the properties of these chlorocarboxylate derivatives has been studied. However, the role of the axial halogen ligand has been little explored. To the best of our knowledge, only one crystal structure of a bromo derivative, which contains zigzag chains, has been described.[20] We have recently published[19] the first crystal structure of an iododiruthenium derivative showing a cation/anion arrangement $[Ru_2(\mu\text{-}O_2CCH_2CH_2OPh)_4(H_2O)_2]$-$[Ru_2I_2(\mu\text{-}O_2CCH_2CH_2OPh)_4]$ in the solid state. The crystal structure of the diiodotetrabenzamidinatodiruthenium(III) complex $[Ru_2(DMBA)_4I_2]$ (DMBA = *N*,*N*′-dimethylbenzamidinate) has been reported very recently.[21]

In this paper we analyse the role of the axial halogen ligand on the properties of the halotetracarboxylatodiruthenium(II,III) complexes. Tetrabenzoate- and tetra-*p*-methoxybenzoatediruthenium(II,III) compounds have been used in this study. The preparation and structural characterization of new bromo and iodo derivatives are described. The synthesis of the bromo and iodo complexes with 2,2-diphenylpropionate has been reported in a previous paper[19] but the structural determination of both complexes is reported here. These complexes show an intense solvatochromism in several solvents, which is also explored.

[a] Departamento de Química Inorgánica, Universidad Complutense
Ciudad Universitaria, 28040 Madrid, Spain
Fax: +34-91-394-4352
E-mail: qcmm@quim.ucm.es
[b] Centro de Asistencia a la Investigación de Rayos X, Facultad de Ciencias Químicas, Universidad Complutense
Ciudad Universitaria, 28040 Madrid, Spain

Results and Discussion

The reaction of $[Ru_2Cl(\mu\text{-}O_2CR)_4]$ (R = Ph, C_6H_4-*p*-OMe) with $AgBF_4$ in THF leads to the complexes $[Ru_2(\mu\text{-}O_2CR)_4(THF)_2]BF_4$, which were treated in ethanol with an aqueous solution of KBr or KI to give $[Ru_2X(\mu\text{-}O_2CPh)_4]_n$ [X = Br (**1**), I (**2**)] and $[Ru_2X(\mu\text{-}O_2CC_6H_4\text{-}p\text{-}OMe)_4(H_2O)]$ [X = Br (**3**) and I (**4**)]. Crystals of **1** and **2** were grown by layering an ethanol solution of $[Ru_2(\mu\text{-}O_2CR)_4(THF)_2]BF_4$ onto an aqueous solution of KX (X = Br, I). An analogous procedure allowed us to isolate single crystals of $[Ru_2Br(\mu\text{-}O_2CCMePh_2)_4(EtOH)]\cdot 0.5EtOH$ (**5**·0.5EtOH). The hydrate $[Ru_2Br(\mu\text{-}O_2CCMePh_2)_4(H_2O)]$ and unsolvated $[Ru_2Br(\mu\text{-}O_2CCMePh_2)_4]$ have been isolated previously, although the growth of single crystals was not possible.[19] The slow evaporation of an ethanol/water solution of compound **3** gave crystals of **3**·H_2O. Crystals of **4**·H_2O were obtained by cooling a methanol solution of **4** to −18 °C. Single crystals of $[Ru_2I(\mu\text{-}O_2CCMePh_2)_4(MeOH)]\cdot 0.5H_2O$ (**6**·0.5H_2O) were grown from a methanol/water solution containing the cation $[Ru_2(\mu\text{-}O_2CCMePh_2)_4]^+$ and tetraphenylphosphonium iodide over 48 h.

The unsolvated $[Ru_2X(\mu\text{-}O_2CR)_4]$ complexes were prepared by heating the solvated complexes under vacuum.

All compounds are thermally stable in air and can be manipulated without decomposition for long periods of time. They are soluble in methanol, DMSO and THF, but insoluble in hexane or toluene, and are 1:1 electrolytes in methanol and DMSO but non-electrolytes in acetone, THF and acetonitrile solutions.[22]

The IR spectra of all compounds exhibit the typical pattern for bridging carboxylate ligands in the CO_2 stretching region.[1−3] Other bands attributable to aryl or alkyl groups of the carboxylate ligands are also observed in all cases. For **3** and **4** bands corresponding to coordinated water molecules also appear.

The base peak in all mass spectra (ESI+) corresponds to the ion $[Ru_2(\mu\text{-}O_2CR)_4]^+$ or $[Ru_2(\mu\text{-}O_2CR)_4(DMSO)]^+$. The $[Ru_2X(\mu\text{-}O_2CR)_4]^+$ ion is only observed in compound **1**. In complex **5**, the molecular peak associated with a DMSO molecule $[Ru_2Br(\mu\text{-}O_2CCMePh_2)_4(DMSO)]^+$ is detected. All spectra in ESI negative mode show the peak corresponding to the ion $[Ru_2X_2(\mu\text{-}O_2CR)_4]^-$.

Crystal Structures of $[Ru_2Br(\mu\text{-}O_2CPh)_4]$ (1), $[Ru_2Br(\mu\text{-}O_2CC_6H_4\text{-}p\text{-}OMe)_4(H_2O)]\cdot H_2O$ (3·H_2O), and $[Ru_2Br(\mu\text{-}O_2CCMePh_2)_4(EtOH)]\cdot 0.5EtOH$ (5·0.5EtOH)

The crystal structures of these complexes are depicted below. Selected bond lengths and angles are given in Table 1. These complexes have two Ru atoms linked by four carboxylate bridging ligands. The Ru−Ru distances are 2.2906(7), 2.2756(17), and 2.2849(14) Å, respectively. These distances are of the same order as those found in other carboxylatodiruthenium(II,III) compounds.[1−3]

The structure of **1** (Figure 1) consists of $[Ru_2(\mu\text{-}O_2CPh)_4]^+$ units connected by bromide ions to give zigzag chains. The Ru−Br−Ru angle of 117.00(3)° is similar to those found in other polymeric complexes,[5,7,9,10,12,15] and in the sole previously described bromo derivative $[Ru_2Br(\mu\text{-}O_2CH)_4]_n$.[20] Figure 2 shows the packing of the zigzag chains in the solid state. No significant interactions are seen between the chains of $[Ru_2Br(\mu\text{-}O_2CPh)_4]_n$.

Table 1. Selected bond lengths (Å) and angles (°) for $[Ru_2Br(\mu\text{-}O_2CPh)_4]$ (**1**), $[Ru_2Br(\mu\text{-}O_2CC_6H_4\text{-}p\text{-}OMe)_4(H_2O)]\cdot H_2O$ (**3**·H_2O), and $[Ru_2Br(\mu\text{-}O_2CCMePh_2)_4(EtOH)]\cdot 0.5EtOH$ (**5**·0.5EtOH); symmetry transformations used to generate equivalent atoms: #1: $-x+2, -y+1, -z$; #2: $-x+2, y, z+1/2$.

1		**3**·H_2O		**5**·0.5EtOH	
Ru(1)−Ru(1)#1	2.2906(7)	Ru(1)−Ru(2)	2.2756(17)	Ru(1)−Ru(2)	2.2849(14)
Ru(1)−Br(1)	2.6700(5)	Ru(1)−Br(1)	2.671(2)	Ru(1)−Br(1)	2.6108(17)
Ru(1)−O(1)	2.014(3)	Ru(1)−O(1)	2.002(10)	Ru(1)−O(2)	2.027(9)
Ru(1)−O(2)	2.025(3)	Ru(1)−O(4)	2.014(10)	Ru(1)−O(4)	2.033(8)
Ru(1)−O(3)	2.018(3)	Ru(1)−O(5)	1.989(9)	Ru(1)−O(7)	2.013(9)
Ru(1)−O(4)	2.023(3)	Ru(1)−O(8)	2.028(11)	Ru(1)−O(9)	2.018(9)
Br(1)−Ru(1)#2	2.670(5)	Ru(2)−O(2)	1.996(9)	Ru(2)−O(1)	2.296(8)
Ru(1)#1−Ru(1)−Br(1)	174.94(3)	Ru(2)−O(3)	1.973(10)	Ru(2)−O(3)	2.024(9)
Ru(1)#2−Br(1)−Ru(1)	117.00(3)	Ru(2)−O(6)	2.017(10)	Ru(2)−O(5)	2.011(9)
O(1)−Ru(1)−Ru(1)#1	89.73(8)	Ru(2)−O(7)	1.998(10)	Ru(2)−O(6)	2.016(8)
O(2)−Ru(1)−Ru(1)#1	89.86(8)	Ru(2)−O(9)	2.292(11)	Ru(2)−O(8)	2.012(9)
O(3)−Ru(1)−Ru(1)#1	86.44(8)	Ru(2)−Ru(1)−Br(1)	177.64(8)	Ru(2)−Ru(1)−Br(1)	178.48(8)
O(4)−Ru(1)−Ru(1)#1	90.42(8)	Ru(1)−Ru(2)−O(9)	177.6(3)	Ru(1)−Ru(2)−O(1)	177.5(3)
		O(1)−Ru(1)−Ru(2)	88.7(3)	O(2)−Ru(1)−Ru(2)	88.9(2)
		O(4)−Ru(1)−Ru(2)	89.0(3)	O(4)−Ru(1)−Ru(2)	88.0(2)
		O(5)−Ru(1)−Ru(2)	89.4(3)	O(7)−Ru(1)−Ru(2)	88.6(2)
		O(8)−Ru(1)−Ru(2)	89.4(3)	O(9)−Ru(1)−Ru(2)	88.8(2)
		O(2)−Ru(2)−Ru(1)	89.7(3)	O(3)−Ru(2)−Ru(1)	89.9(2)
		O(3)−Ru(2)−Ru(1)	90.4(3)	O(5)−Ru(2)−Ru(1)	90.3(2)
		O(6)−Ru(2)−Ru(1)	90.4(3)	O(6)−Ru(2)−Ru(1)	89.8(2)
		O(7)−Ru(2)−Ru(1)	89.8(3)	O(8)−Ru(2)−Ru(1)	89.7(2)
				C(61)−O(1)−Ru(2)	134.5(10)

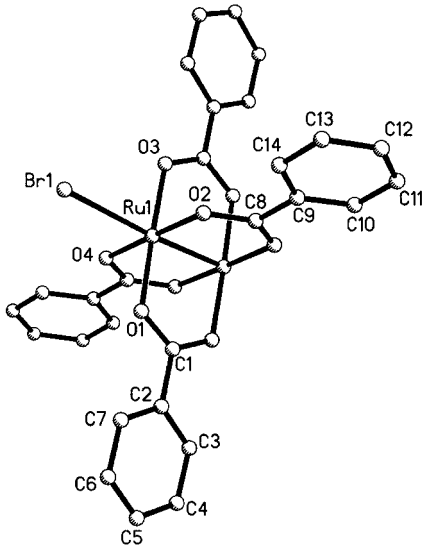

Figure 1. PLUTO view of $[Ru_2Br(\mu\text{-}O_2CPh)_4]$ (**1**); hydrogen atoms have been omitted for clarity

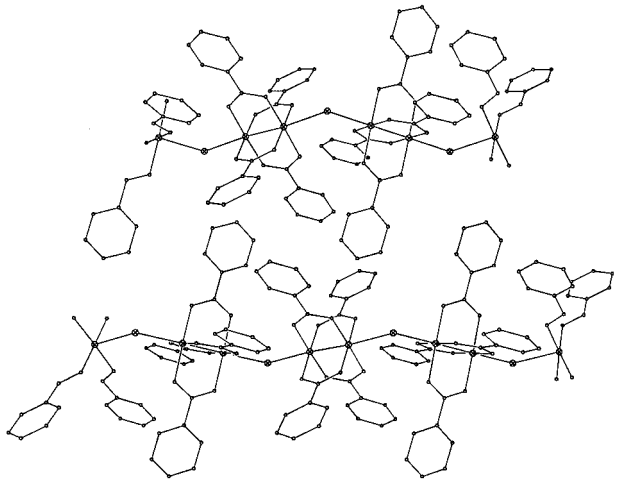

Figure 2. Packing of the polymeric complex **1**

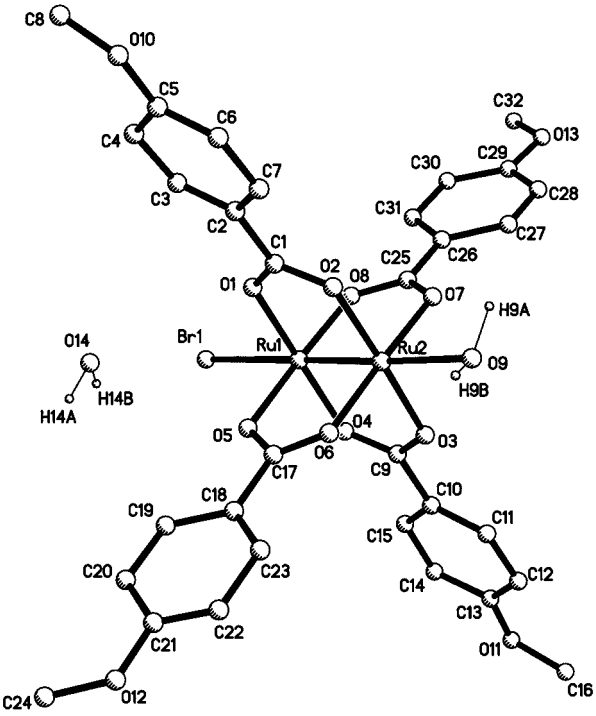

Figure 3. PLUTO view of $[Ru_2Br(\mu\text{-}O_2CC_6H_4\text{-}p\text{-}OMe)_4(H_2O)]\cdot H_2O$ (**3**·H_2O); hydrogen atoms, except in water molecules, have been omitted for clarity

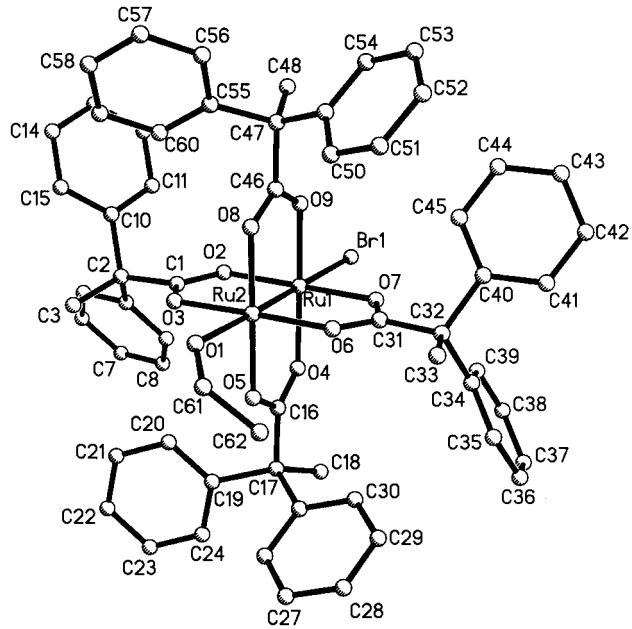

Figure 4. PLUTO view of $[Ru_2Br(\mu\text{-}O_2CCMePh_2)_4(EtOH)]\cdot 0.5EtOH$ (**5**·0.5EtOH); crystallization solvent molecules and hydrogen atoms have been omitted for clarity

The molecular structures of complexes **3**·H_2O (Figure 3) and **5**·0.5EtOH (Figure 4) consists of discrete dinuclear molecules of $[Ru_2Br(\mu\text{-}O_2CR)_4(S)]$ (S = solvent molecule). The dinuclear unit of **3**·H_2O has one bromide atom and one water molecule in the axial positions. The crystallisation water molecule is hydrogen bonded to the coordinated water of a dinuclear unit and to the bromide ligand of another dimetallic molecule. The molecular structure of **5**·0.5EtOH is similar, with one of the axial positions occupied by an ethanol molecule instead of a water molecule. In this compound, the possible presence of hydrogen bonds could not be established due to the low quality of the crystal.

The molecular nature of these bromo derivatives contrasts with the polymeric chains found in the formate derivative[20] and with the above-described benzoate complex **1**. The formation of discrete dinuclear molecules in **3**·H_2O

in the solid state is more surprising because all chloro derivatives with arenecarboxylate ligands,[1−3] including the *p*-methoxybenzoate complex[9] $[Ru_2Cl(\mu\text{-}O_2CC_6H_4\text{-}p\text{-}OMe)_4]_n$, have a polymeric structure. Complexes **3**·H_2O and **5**·0.5EtOH are the first examples of halotetraarenecarboxylatodiruthenium(II,III) compounds with a nonpolymeric arrangement. This molecular nature indicates that the axial ligands play a key role in the arrangement of these diruthenium(II,III) complexes in the solid state.

The Ru−Br bond lengths for **1**, **3**·H_2O, and **5**·0.5EtOH are 2.6700(5), 2.671(2), and 2.6108(17) Å, respectively. In the molecular complex **5**·0.5EtOH the Ru−Br bond length is shorter than in the polymeric compound **1** and in $[Ru_2Br(\mu\text{-}O_2CH)_4]_n$ [2.7170(8)−2.7313(9) Å].[20] This fact is consistent with the variation observed in the Ru−Cl distances in the analogous molecular and polymeric chlorotetracarboxylatodiruthenium(II,III) complexes.[4−19] However, the Ru−Br distance in the molecular compound **3**·H_2O is slightly longer than in polymeric **1**.

Crystal Structures of $[Ru_2I(\mu\text{-}O_2CPh)_4]$ (2), $[Ru_2I(\mu\text{-}O_2CC_6H_4\text{-}p\text{-}OMe)_4(H_2O)]\cdot H_2O$ (4·H_2O), and $[Ru_2I(\mu\text{-}O_2CCMePh_2)_4(MeOH)]\cdot 0.5H_2O$ (6·0.5H_2O)

Figure 5 shows a PLUTO view of the dinuclear unit of **2**. Selected bond lengths and angles are collected in Table 2. The arrangement in the solid state — zigzag chains with an iodide ligand linking the $[Ru_2(\mu\text{-}O_2CPh)_4]^+$ units — is similar to that found in **1**. The chains are separated by normal van der Waals forces. The Ru−I−Ru angle is 114.246(18)° and the Ru−I distance [2.8562(4) Å] is longer than the Ru−Br distance [2.6700(5) Å] in **1**. This large bond length is in accordance with the size of the axial ligand. The Ru−Ru distance [2.2965(6) Å] is longer than those observed in the chloro derivatives [2.267(1)−2.292(7) Å]. It is independent of the type of arrangement in the solid state[4−19] and is similar to that found[19] in $[Ru_2(\mu\text{-}O_2CCH_2CH_2OPh)_4(H_2O)_2][Ru_2I_2(\mu\text{-}O_2CCH_2CH_2OPh)_4]$ [2.310(2) Å].

Complexes **4**·H_2O (Figure 6) and **6**·0.5H_2O (Figure 7) have molecular structures analogous to those of **3**·H_2O and **5**·0.5EtOH. Selected bond lengths and angles are listed in Table 2. The structural parameters of the $[Ru_2(\mu\text{-}O_2C)_4]$ units are similar in the four complexes. In compounds **4**·H_2O and **6**·0.5H_2O one axial position is occupied by an iodide ligand and the other one is occupied by a water molecule or a MeOH ligand, respectively. In complex **4**·H_2O the water molecule of crystallization is hydrogen bonded to the coordinated water of a dinuclear unit and to the bromide ligand of another dimetallic molecule, similarly to **3**·H_2O. The Ru−I bond lengths in **4**·H_2O and **6**·0.5H_2O are 2.831(4) and 2.8055(10) Å, respectively, which are shorter than that observed for compound **2**. The Ru−I distances in these tetracarboxylatodiruthenium(II,III) derivatives are also shorter than those found in the benzamidinatediruthenium(III) complex[21] $[Ru_2I_2(DMBA)_4]$ [2.917(1) and 2960(1) Å].

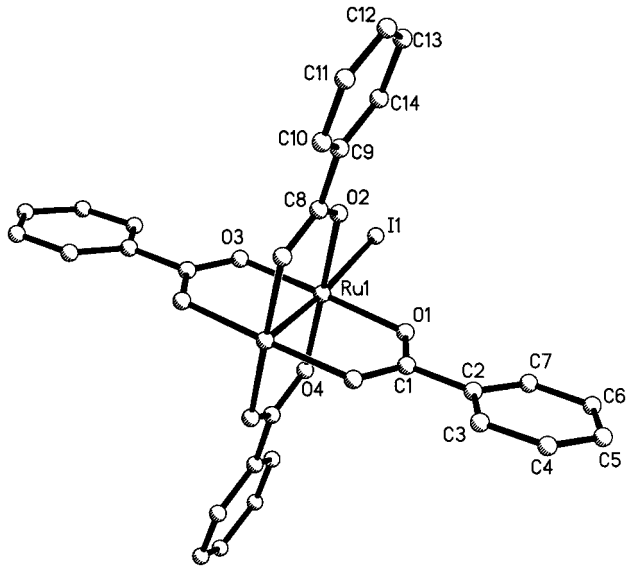

Figure 5. PLUTO view of $[Ru_2I(\mu\text{-}O_2CPh)_4]$ (**2**); hydrogen atoms have been omitted for clarity

Magnetic Properties

Magnetic measurements of the compounds show magnetic moments at room temperature of 4.09−4.36 μ_B in all cases. These values correspond to the presence of three unpaired electrons per dimer unit, in accordance with the ground-state configuration $\sigma^2\pi^4\delta^2(\pi^*\delta^*)^3$ proposed by Norman et al.[23] In all cases the molar magnetic susceptibility increases with decreasing temperature and no maximum is observed. The magnetic moments of these complexes decrease with temperature. This behaviour is usual in this type of complexes and has been ascribed[11,13,15,19,24−27] to a large zero-field splitting (ZFS) and some degree of antiferromagnetic coupling between the dimetallic units. The zero-field splitting effect on the susceptibility can be quantified by considering the Hamiltonian $H_D = S\cdot D\cdot S$, as described by O'Connor.[28] The perturbation of a weak antiferromagnetic coupling over the zero-field splitting system can be considered by using the molecular field approximation.[28] Thus, for an $S = 3/2$ spin system the magnetic suscpetibility can be expressed as:

$$\chi' = \chi'_M/[1 - (2zJ/Ng^2\beta^2)\chi'_M]$$

where χ'_M includes the temperature independent paramagnetism (TIP)

$$\chi'_M = \chi_M + \text{TIP}$$

and

$\chi_M = (\chi_\parallel + 2\chi_\perp)/3$,
$\chi_\parallel = (Ng^2\beta^2/kT)(1 + 9e^{-2D/kT})/4(1 + e^{-2D/kT})$ and
$\chi_\perp = (Ng^2\beta^2/kT)[4 + (3kT/D)(1 - e^{-2D/kT})]/4(1 + e^{-2D/kT})$.

Finally, the consideration of a paramagnetic impurity (P) leads to the expression

$$\chi'_{mol} = [(1 - P)\chi'] + [PNg^2_{mo}\beta^2/4kT]$$

which has been used previously[13,15,19] in the fits of similar diruthenium complexes.

Table 2. Selected bond lengths (Å) and angles (°) for $[Ru_2I(\mu\text{-}O_2CPh)_4]$ (**2**), $[Ru_2I(\mu\text{-}O_2CC_6H_4\text{-}p\text{-}OMe)_4(H_2O)]\cdot H_2O$ (**4**·H_2O), and $[Ru_2I(\mu\text{-}O_2CCMePh_2)_4(MeOH)]\cdot 0.5H_2O$ (**6**·$0.5H_2O$); symmetry transformations used to generate equivalent atoms: #1: $-x + 1, -y + 1, -z + 1$; #2: $-x + 1, y, -z + 1/2$.

2		**4**·H_2O		**6**·$0.5H_2O$	
Ru(1)−Ru(1)#1	2.2965(6)	Ru(2)−Ru(1)	2.273(3)	Ru(1)−Ru(2)	2.2902(11)
Ru(1)−I(1)	2.8562(4)	Ru(1)−I(1)	2.831(4)	Ru(2)−I(1)	2.8055(10)
Ru(1)−O(1)	2.018(3)	Ru(1)−O(1)	2.00(2)	Ru(1)−O(1)	2.010(6)
Ru(1)−O(2)	2.023(2)	Ru(1)−O(4)	2.032(19)	Ru(1)−O(4)	2.021(6)
Ru(1)−O(3)	2.021(3)	Ru(1)−O(5)	2.007(19)	Ru(1)−O(6)	1.999(6)
Ru(1)−O(4)	2.023(2)	Ru(1)−O(8)	1.987(19)	Ru(1)−O(7)	2.014(6)
I(1)−Ru(1)#2	2.8562(4)	Ru(2)−O(2)	1.99(2)	Ru(1)−O(17)	2.314(8)
Ru(1)#1−Ru(1)−I(1)	174.71(2)	Ru(2)−O(3)	2.00(2)	Ru(2)−O(2)	2.042(6)
Ru(1)−I(1)−Ru(1)#2	114.246(18)	Ru(2)−O(6)	1.970(18)	Ru(2)−O(3)	2.038(6)
O(1)−Ru(1)−Ru(1)#1	89.70(8)	Ru(2)−O(7)	1.964(17)	Ru(2)−O(5)	2.039(6)
O(2)−Ru(1)−Ru(1)#1	88.51(8)	Ru(2)−O(9)	2.288(19)	Ru(2)−O(8)	2.050(6)
O(3)−Ru(1)−Ru(1)#1	88.45(8)	Ru(2)−Ru(1)−I(1)	176.87(15)	Ru(1)−Ru(2)−I(1)	176.68(4)
O(4)−Ru(1)−Ru(1)#1	89.81(8)	O(9)−Ru(2)−Ru(1)	178.0(5)	Ru(2)−Ru(1)−O(17)	177.64(19)
		O(1)−Ru(1)−Ru(2)	88.1(6)	O(1)−Ru(1)−Ru(2)	90.31(19)
		O(4)−Ru(1)−Ru(2)	87.8(6)	O(4)−Ru(1)−Ru(2)	90.18(19)
		O(5)−Ru(1)−Ru(2)	87.3(6)	O(6)−Ru(1)−Ru(2)	89.37(19)
		O(8)−Ru(1)−Ru(2)	90.4(6)	O(7)−Ru(1)−Ru(2)	90.5(2)
		O(2)−Ru(2)−Ru(1)	90.3(6)	O(2)−Ru(2)−Ru(1)	87.59(19)
		O(3)−Ru(2)−Ru(1)	88.8(7)	O(3)−Ru(2)−Ru(1)	88.2(2)
		O(6)−Ru(2)−Ru(1)	90.7(6)	O(5)−Ru(2)−Ru(1)	88.53(19)
		O(7)−Ru(2)−Ru(1)	90.7(6)	O(8)−Ru(2)−Ru(1)	87.68(19)
				C(121)−O(17)−Ru(1)	125.5(8)

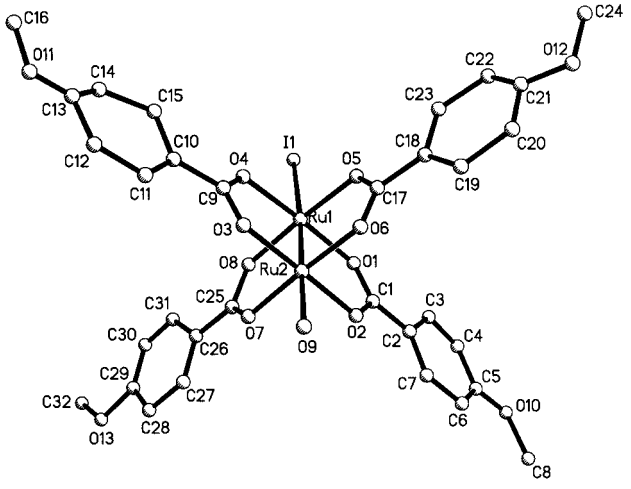

Figure 6. PLUTO view of $[Ru_2I(\mu\text{-}O_2CC_6H_4\text{-}p\text{-}OMe)_4(H_2O)]\cdot H_2O$ (**4**·H_2O); crystallization solvent molecules and hydrogen atoms have been omitted for clarity

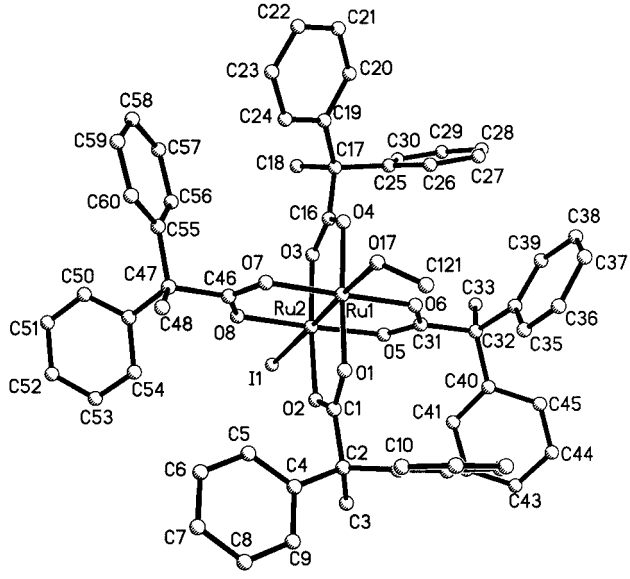

Figure 7. PLUTO view of $[Ru_2I(\mu\text{-}O_2CCMePh_2)_4(MeOH)]\cdot 0.5H_2O$ (**6**·$0.5H_2O$); crystallization solvent molecules and hydrogen atoms have been omitted for clarity

The magnetic parameters obtained in the fit of the magnetic data of complexes **1**−**4** using this model are collected in Table 3. The magnetic properties of complexes **5**·0.5EtOH and **6**·$0.5H_2O$ are analogous to those described previously[19] for $[Ru_2X(\mu\text{-}O_2CCMePh_2)_4(H_2O)]$ (X = Br, I).

A very good agreement between the experimental and calculated curves of the magnetic moment and the molar susceptibility for complexes **1**−**4** was observed. Figure 8 shows the experimental and calculated curves for complex **1** using the above-mentioned model. Similar curves have been obtained for the other complexes, with *D* values ranging from 63.4 to 71.5 cm^{-1}. Similar *D* values have been calculated for other tetracarboxylato complexes.[13,15,19] These large *D* values are a consequence of the presence of two second row transition metal atoms and the existence of several vacant energy levels near the HOMO level in the diruthenium unit, as described by Norman et al.[23] The *zJ* values for complexes **3** and **4** are low as is expected from their molecular nature. Low *zJ* values are also observed in **1** and **2,** as expected for polymeric complexes with Ru−X−Ru angles lower than 125°.[13,15,19] The higher *zJ* value of the bromo complex **1** with respect to the iodo complex **2** could

Table 3. Magnetic parameters obtained in the fits of the magnetic moment as a function of temperature

Compound	g	D (cm^{-1})	zJ (cm^{-1})	TIP (mL/mol)	P (%)	$\sigma^{2[a]}$
1	2.16	63.4	−1.37	$3.46\ 10^{-4}$	0.08	8.80×10^{-6}
2	2.15	71.5	−0.03	$<10^{-6}$	2.67×10^{-3}	3.27×10^{-5}
3·H_2O	2.30	70.0	−0.04	$<10^{-6}$	0.03	8.10×10^{-4}
4·H_2O	2.35	70.0	−0.04	$<10^{-6}$	8.80×10^{-3}	4.93×10^{-4}

[a] $\sigma^2 = \Sigma(\mu_{eff.calcd.} - \mu_{eff.exp.})^2/\Sigma\mu_{eff.exp.}^2$.

be due to the better overlap between the π-type lone-pair orbital of the bromo ligand and the π*(Ru−Ru) orbital as the overlapping of the π-type halogen and ruthenium orbitals in these complexes becomes smaller for the heavier halide ligand.

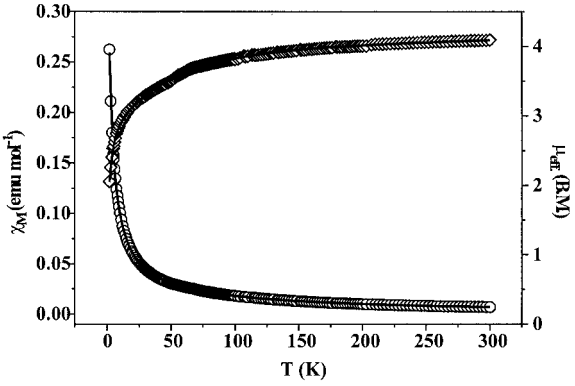

Figure 8. Temperature dependence of the molar susceptibility χ_M (circles) and $\mu_{eff.}$ (rhombs) for complex **1**; solid lines are the product of a least-squares fit to the model indicated in the text

Electronic Properties

The absorption data in the visible-UV−NIR range for solutions of complexes **1**−**6** in several solvents are given in Table 4.

The electronic spectra of the complexes in methanol solution mainly show two bands in the visible-UV range at about 430 and 330 nm. The major absorption band in the visible range (430 nm) is unambiguously assigned to a π(RuO,Ru_2) → π*(Ru_2) transition according to Norman et al.[23] and Miskowski and Gray.[29] The metal-metal character ($Ru_2 \rightarrow Ru_2$) of this transition has been well established by resonance Raman studies[29,30] although the amount of ligand to metal charge transfer (LMCT) (RuO → Ru_2) seems to be questionable. The band observed at ca. 330 nm could be assigned to a ligand-to-metal charge transfer π(axial ligand) → π*(Ru_2) transition. This assignment is in accordance with that described previously for other tetracarboxylatodiruthenium(II,III) complexes.[1,3,29]

The complexes **1**−**6** are 1:1 electrolytes in MeOH and DMSO solutions. As a consequence, the cation [Ru_2(μ-O_2CR)$_4$(S)$_2$]$^+$ (S = solvent) is present in solution and no dependence on the nature of the halogen is observed. However, the conductivity measurements in acetone, acetonitrile and THF indicate that these complexes are nonelectrolytes and the monoadducts [Ru_2X(μ-O_2CR)$_4$(S)] must exist in solution.

In order to compare the electronic spectra of this series of chloro-, bromo-, and iodotetracarboxylatodiruthenium(II,III) derivatives, the UV/Vis-NIR data of the chloro compounds [Ru_2Cl(μ-O_2CR)$_4$] (R = C_6H_4-*p*-OMe, $CMePh_2$) were also recorded (Table 4). However, the spectra of the chlorotetrabenzoate complex was not measured due to its insolubility.

The first absorption band observed in the chloro complexes in the range 317−339 nm could be assigned to an LMCT π(axial ligand) → π*(Ru_2) transition similar to that described above for the [Ru_2(μ-O_2CR)$_4$(MeOH)$_2$]$^+$ species. This band is shifted to 340−400 nm and to 409−445 nm in the bromo and iodo complexes, respectively. This assignment is in accordance with the sensibility of this transition to the axial ligand and with the strong, systematic red shift predicted for the change from chloro to iodo. An analogous shift has been described in the UV/Vis spectra of the dibromo and diiodo complexes[29] (Bu_4N)[Ru_2Br_2(μ-O_2CPr)$_4$] and (Bu_4N)[Ru_2I_2(μ-O_2CPr)$_4$]. The first high-intensity absorption observed in the iodo complexes in the range 344−383 nm could be assigned to an LMCT σ(axial ligand) → σ*(Ru_2) transition, in agreement with those described[29] for the 307 nm band observed in the diodo anion [Ru_2I_2(μ-O_2CR)$_4$]$^-$.

The second absorption band observed in the chloro complexes in the range 464−467 nm is assigned to the π(RuO,Ru_2) → π*(Ru_2) transition. This absorption is slightly red-shifted in the bromo derivatives (476−494 nm), whereas in the iodo compounds it is strongly shifted (564−625 nm). This absorption should be only very weakly sensitive to the nature of the axial ligand,[1,3,29] although it has been described that in the diiodo complex (Bu_4N)-[Ru_2I_2(μ-O_2CPr)$_4$] it is strongly perturbed. This perturbation could be due to the mixing of this transition with the π(axial ligand) → π*(Ru_2) charge transfer.[29] Figure 9 shows the electronic spectra of the 2,2-diphenylpropionato derivatives [Ru_2X(μ-O_2CC$Me Ph_2$)$_4$] (X = Cl, Br, I) in acetone.

The chloro and bromo derivatives also display a very weak shoulder in the range 553−622 nm which is shifted to 712−754 nm in the iodo compounds. This band could be assigned to a σ(Ru-axial ligand) → π*(Ru_2) transition in accordance with the very weak and poorly defined band at ca. 560 nm observed in some chloro complexes [Ru_2Cl(μ-O_2CR)$_4$].[8,23,29]

All the complexes show a weak absorption band in the range 981−1166 nm in the NIR region due to the δ → δ* transition.

Table 4. Electronic spectra data for $[Ru_2X(\mu\text{-}O_2CR)_4]$

Compound R	X		λ (nm) (ε; $dm^3 \cdot mol^{-1} \cdot cm^{-1}$) σ(axial ligand) → σ*($Ru_2$)	π(axial ligand) → π*(Ru_2)	π(RuO,Ru_2) → π*(Ru_2)	σ(axial ligand) → π*(Ru_2)	δ(Ru_2) → δ*(Ru_2)
			MeOH				
Ph	Br	**1**		335 sh (3032)	434 (743)	523 sh (118)	1040 (52)
	I	**2**		333 sh (3074)	433 (715)	522 sh (188)	1012 (49)
C_6H_4-*p*-OMe	Cl	[a]		385 sh (1233)	427 (786)		1092 (48)
	Br	**3**		358 sh (1637)	427 (552)		1108 (31)
	I	**4**		372 sh (2076)	425 (1125)		1105 (69)
$CMePh_2$	Cl	[b]		335 (1325)	425 (983)	533 sh (263)	987 (34)
	Br	**5**		336 sh (1024)	425 (807)	531 sh (200)	988 (32)
	I	**6**		335 sh (1024)	425 (850)	531 sh (254)	986 (52)
			DMSO				
Ph	Br	**1**		336 sh (4239)	438 (1011)	564 (528)	994 (84)
	I	**2**		333 sh (5355)	437 (1020)	561 (493)	995 (52)
C_6H_4-*p*-OMe	Cl	[a]		386 sh (1469)	444 (930)	562 sh (293)	1137 (32)
	Br	**3**		384 sh (1579)	439 (982)	542 sh (364)	1125 (37)
	I	**4**		370 sh (2515)	441 (1251)	552 sh (397)	1166 (53)
$CMePh_2$	Cl	[b]		324 (2261)	438 (1104)	562 (553)	1040 (47)
	Br	**5**		320 sh (2153)	438 (1081)	557 (379)	1033 (46)
	I	**6**		320 sh (2191)	438 (1050)	557 (344)	986 (35)
			Acetone				
Ph	Br	**1**	insoluble				
	I	**2**	344 sh (5056)	419 (2071)	593 (2142)	737 sh (373)	1153 (106)
C_6H_4-*p*-OMe	Cl	[a]	insoluble				
	Br	**3**	insoluble				
	I	**4**	383 sh (2605)	412 sh (2282)	579 (2027)	712 sh (363)	1153 (96)
$CMePh_2$	Cl	[b]		329 (6718)	464 (2012)	595 sh (468)	1065 (105)
	Br	**5**		370 (3722)	483 (2230)	602 sh (407)	1097 (157)
	I	**6**	349 sh (3849)	418 (2796)	599 (2673)	718 sh (726)	1102 (228)
			THF				
Ph	Br	**1**		377 (3127)	492 (1772)	619 sh (182)	981 (50)
	I	**2**	347 sh (10252)	409 sh (3086)	625 (1577)	738 sh (360)	960 sh (83)
C_6H_4-*p*-OMe	Cl	[a]			467 (2376)	581 sh (433)	1169 (83)
	Br	**3**		366 (4359)	490 (1884)	604 sh (274)	1160 (54)
	I	**4**	354 sh (7680)	418 sh (3016)	612 (2510)	754 sh (395)	1000 (82)
$CMePh_2$	Cl	[b]		339 (3521)	465 (1182)	577 sh (249)	1073 (106)
	Br	**5**		381 (3367)	494 (2512)	622 sh (256)	1093 (59)
	I	**6**	366 (5351)	444 sh (1230)	614 (400)		1113 (35)
			CH_3CN				
Ph	Br	**1**	insoluble				
	I	**2**	348 (6065)		573 (1861)		
C_6H_4-*p*-OMe	Cl	[a]	insoluble				
	Br	**3**		347 sh (4634)	476 (1241)	576 sh (453)	1161 (61)
	I	**4**	348 sh (4399)	445 sh (1145)	564 (1413)		1151 (92)
$CMePh_2$	Cl	[b]		317 (4659)	464 (1215)	553 sh (664)	
	Br	**5**		363 (2731)	477 (1479)	565 sh (532)	1102 (64)
	I	**6**	356 (4396)	409 sh (2075)	585 (1517)		1108 (67)

[a] $[Ru_2Cl(\mu\text{-}O_2CC_2H_4\text{-}p\text{-}OMe)_4]$. [b] $[Ru_2Cl(\mu\text{-}O_2CCMePh_2)_4]$.

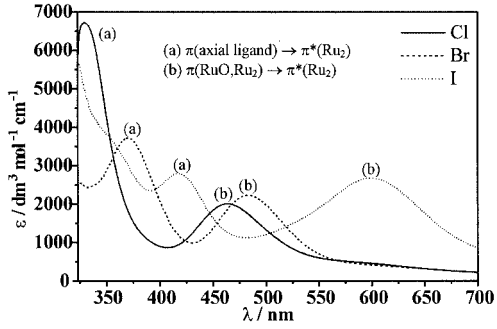

Figure 9. Electronic spectra of $[Ru_2X(\mu\text{-}O_2CCMePh_2)_4]$ in acetone

The variations in the absorption bands imply important colour changes of the solutions of the complexes. All compounds are yellow in methanol or DMSO solutions, due to the existence of the π(RuO,Ru_2) → π*(Ru_2) transition in the visible range. The acetonitrile, acetone, and THF solutions of the chloro derivatives have a similar yellow-brown colour and the bromo derivatives show a little solvatochromism, whose colours change from yellow-orange to pink. However, the iodo derivatives in acetone, acetonitrile and THF are blue, violet, and green respectively. The $[Ru_2I(\mu\text{-}O_2CR)_4(S)]$ complexes display two transitions in the visible range, but the colour changes seems to be related mainly

with the presence, position, and intensity of the second band, in which the axial ligands have a great influence. In summary, the electronic data of the halotetracarboxylatodiruthenium(II,III) complexes indicate that the solvatochromism of these complexes can be ascribed to the combined influence of the halide and the solvent molecule bonded to the axial positions.

Conclusions

In this work we have found that complexes of the type $[Ru_2X(\mu\text{-}O_2CR)_4]$ (X = Br, I) give polymeric zigzag chains with R = Ph and discrete dinuclear molecules with R = C_6H_4-*p*-OMe or $CMePh_2$ ligands. These examples represent the first nonpolymeric complexes with arenecarboxylate bridging ligands, and indicate that the polymeric or molecular nature of this type of compounds is due to the influence of the equatorial and axial ligands. The presence of chloride, bromide or iodide as axial ligand in the diruthenium complexes produce a shift of the LMCT bands to lower energy. In the iodo derivatives a strong shift of the $\pi(RuO,Ru_2) \rightarrow \pi^*(Ru_2)$ transition is also induced, thereby producing solvatochromism for these complexes.

Experimental Section

General Remarks: All reactions were carried out under an inert atmosphere, using standard Schlenk techniques. Ruthenium trichloride, carboxylic acids and solvents were obtained from commercial sources and used without previous purification. The complexes $[Ru_2Cl(\mu\text{-}O_2CR)_4]$ (R = C_6H_4-*p*-OMe, $CMePh_2$, Ph) were prepared by literature procedures.[9,11,31] IR spectra were recorded as KBr discs on a Nicolet Magna-FTIR 550 spectrophotometer. Elemental analysis of C and H were performed by the Microanalytical Service of the Complutense University of Madrid. Electronic spectra in the range 250−1300 nm were recorded on a Cary 5G spectrophotometer in 10^{-4} M solutions in methanol, DMSO, acetone, THF, or acetonitrile. The variable-temperature magnetic susceptibility data were measured on a Quantum Design MPMSXL SQUID (Superconducting Quantum Interference Device) susceptometer over a temperature range of 2 to 300 K. Each raw data point was corrected for the diamagnetic contribution of both the sample holder and the compound to the susceptibility. The molar diamagnetic corrections for the complexes were calculated on the basis of Pascal's constants. The fits of experimental data were carried out using the commercial MATLAB V.5.1.0.421 program. Mass spectra were obtained on a Bruker Esquire-LC with Electrospray Ionization (ESI) using chloroform, methanol, THF, or DMSO as solvent. Nominal molecular masses and isotopic distributions of all peaks were calculated with the MASAS[32] computer program,

Table 5. Crystal data for $[Ru_2Br(\mu\text{-}O_2CPh)_4]$ (**1**), $[Ru_2Br(\mu\text{-}O_2CC_6H_4\text{-}p\text{-}OMe)_4(H_2O)]\cdot H_2O$ (**3**·H_2O), and $[Ru_2Br(\mu\text{-}O_2CCMePh_2)_4(EtOH)]\cdot 0.5EtOH$ (**5**·0.5EtOH)

	1	**3**·H_2O	**5**·0.5EtOH
Empirical formula	$C_{28}H_{20}BrO_8Ru_2$	$C_{32}H_{32}BrO_{14}Ru_2$	$C_{63}H_{60}BrO_{9.5}Ru_2$
Molecular mass	766.49	922.63	1251.16
Crystal system	monoclinic	tetragonal	monoclinic
Space group	*C*2/*c*	$P4_32_12$	$P2_1/n$
a (Å)	20.9722(16)	15.8370(6)	14.6671(11)
b (Å)	10.9455(9)	15.8370(6)	23.2288(18)
c (Å)	13.1733(10)	30.2980(15)	17.7816(13)
a (°)	90	90	90
β (°)	108.9060(10)	90	103.364(2)
γ (°)	90	90	90
Volume (Å^3)	2860.8(4)	7599.1(6)	5894.1(8)
Z	4	8	4
$D_{calcd.}$ (g cm^{-3})	1.780	1.613	1.410
μ (mm^{-1})	2.499	1.908	1.245
F(000)	1500	3672	2548
Crystal size (mm^3)	0.06 × 0.11 × 0.13	0.10 × 0.34 × 0.37	0.07 × 0.15 × 0.20
θ range (°)	2.05 to 25.00	1.45 to 25.00	1.47 to 25.00
Index ranges	$-24 \le h \le 13$	$-18 \le h \le 16$	$-17 \le h \le 15$
	$-13 \le k \le 12$	$16 \le k \le 18$	$27 \le k \le 27$
	$-15 \le l \le 15$	$36 \le l \le 35$	$21 \le l \le 18$
Collected reflections	7310	40017	30716
Independent reflections	2500 [*R*(int) = 0.0521]	6706 [*R*(int) = 0.1394]	10358 [*R*(int) = 0.1270]
Completeness to θ = 25.00° (%)	99.5	100.0	99.7
Absorption correction	none	none	none
Refinement method	full-matrix least-squares on F^2	full-matrix least-squares on F^2	full-matrix least-squares on F^2
Data/restraints/parameters	2500/0/177	6706/0/438	10358/8/258
Goodness-of-fit on F^2	0.910	1.048	0.993
Final *R* values [$I > 2\sigma(I)$]	*R*1 = 0.0320, *wR*2 = 0.0549	*R*1 = 0.0645, *wR*2 = 0.1686	*R*1 = 0.0908, *wR*2 = 0.2470
R values (all data)	*R*1 = 0.0529, *wR*2 = 0.0597	*R*1 = 0.1628, *wR*2 = 0.2164	*R*1 = 0.2053, *wR*2 = 0.2983
Largest diff. peak/hole (e·Å^{-3})	0.516 and −0.497	1.785 and −0.633	1.925 and −1.092

using a polynomial expansion based on natural abundances of the isotopes.

Preparation of [$Ru_2Br(\mu\text{-}O_2CPh)_4$] (1): Silver tetrafluoroborate (0.07 g, 0.35 mmol) was added to a suspension of [$Ru_2Cl(\mu\text{-}O_2CPh)_4$] (0.25 g, 0.35 mmol) in THF (30 mL). The reaction mixture was stirred for 24 h, giving a solid precipitate of AgCl and a brown solution. The precipitate was filtered through celite and the solution was pumped to dryness. The solid was dissolved in ethanol (10 mL) and treated with a water solution (10 mL) of KBr (0.42 g, 3.50 mmol) giving a light brown precipitate, which was filtered off, washed with water (3 × 20 mL) and dried under vacuum. Single crystals were obtained by slow interdiffusion of the above-mentioned ethanol solution and the aqueous solution of KBr. Yield 0.16 g (59%). $C_{28}H_{20}BrO_8Ru_2$ (766.52): calcd. C 43.88, H 2.63; found C 43.80, H 2.69. IR (KBr): $\tilde{\nu}$ = 3067 w, 3050 w, 1600 m, 1495 m, 1465 s, 1408 vs, 1177 w, 1143 w, 1081 w, 1002 w, 845 w, 715 s, 689 s, 531 m cm^{-1}. $\mu_{eff.}$ = 4.09 μ_B at room temperature. MS in DMSO/MeOH (ESI^+): *m*/*z* = 767 [M^+], 688 [$M^+ - Br$]; (ESI^-): *m*/*z* = 848 [$M^- + Br$].

Preparation of [$Ru_2I(\mu\text{-}O_2CPh)_4$] (2): The reaction was carried out as mentioned above for **1**, using KI (0.58 g, 3.50 mmol) instead of KBr. Yield 0.16 g (57%). $C_{28}H_{20}IO_8Ru_2$ (813.51): calcd. C 41.34, H 2.48; found C 41.20, H 2.45. IR (KBr): $\tilde{\nu}$ = 3066 w, 1600 m, 1495 m, 1464 s, 1408 vs, 1176 w, 1143 w, 1071 w, 1002 w, 845 w, 715 s, 689 s, 529 m cm^{-1}. $\mu_{eff.}$ = 4.16 μ_B at room temperature. MS in THF/$CHCl_3$ (ESI^+): *m*/*z* = 688 [$M^+ - I$]; (ESI^-): *m*/*z* = 942 [$M^- + I$].

Preparation of [$Ru_2Br(\mu\text{-}O_2CC_6H_4\text{-}p\text{-}OMe)_4(H_2O)$] (3): The reaction was carried out as described above for **1**, using [$Ru_2Cl(\mu\text{-}O_2CC_6H_4\text{-}p\text{-}OMe)_4$] (0.29 g, 0.35 mmol). The solid isolated was characterized as **3**. Single crystals of **3**·H_2O were obtained by evaporation in air of a solution of **3** in methanol. Yield 0.22 g (69%). $C_{32}H_{30}BrO_{13}Ru_2$ (904.64): calcd. C 42.49, H 3.34; found C 42.40, H 3.27. IR (KBr): $\tilde{\nu}$ = 3447 w, 3015 w, 2960 w, 2935 w, 2838 w, 1605 s, 1583 w, 1442 m, 1396 vs, 1315 w, 1304 w, 1261 s, 1172 s, 1109 w, 1025 w, 849 w, 773 m, 702 w, 649 m, 527 w, 511 w, 459 w cm^{-1}. $\mu_{eff.}$ = 4.12 μ_B at room temperature. MS in $CHCl_3$ (ESI^+): *m*/*z* = 808 [$M^+ - Br - H_2O$]; (ESI^-): *m*/*z* = 968 [$M^- + Br - H_2O$].

Preparation of [$Ru_2I(\mu\text{-}O_2CC_6H_4\text{-}p\text{-}OMe)_4(H_2O)$] (4): The reaction was carried out as described above for **2**, using [$Ru_2Cl(\mu\text{-}O_2CC_6H_4\text{-}p\text{-}OMe)_4$] (0.29 g, 0.35 mmol). The brown-violet solid obtained in this way was characterized as **4**. Single crystals of **4**·H_2O were obtained by dissolving **4** in hot methanol (20 mL) and allowing this solution to stand at room temperature and then at −18 °C. Yield 0.21 g (64%). $C_{32}H_{30}IO_{13}Ru_2$ (951.63): calcd. C 40.39, H 3.18; found C 40.26, H 3.08. IR (KBr): $\tilde{\nu}$ = 3447 w, 3078 w, 3013 w, 2961 w, 2934 w, 2837 w, 1605 vs, 1583 m, 1442 s, 1393 vs, 1315 m, 1303 m, 1260 vs, 1172 vs, 1109 w, 1026 m, 849 m, 773 s, 702 w, 668 m, 649 m, 529 w, 511 w, 458 w cm^{-1}. $\mu_{eff.}$ = 4.36 μ_B at room

Table 6. Crystal data for [$Ru_2I(\mu\text{-}O_2CPh)_4$] (**2**), [$Ru_2I(\mu\text{-}O_2CC_6H_4\text{-}p\text{-}OMe)_4(H_2O)$]·$H_2O$ [**4**·H_2O], and [$Ru_2I(\mu\text{-}O_2CCMePh_2)_4(MeOH)$]·0.5$H_2O$ [**6**·0.5H_2O].

	2	**4**·H_2O	**6**·0.5H_2O
Empirical formula	$C_{28}H_{20}IO_8Ru_2$	$C_{32}H_{28}IO_{14}Ru_2$	$C_{63}H_{60}BrO_{9.50}Ru_2$
Molecular weight	813.48	965.58	1251.16
Crystal system	monoclinic	tetragonal	monoclinic
Space group	*C*2/*c*	$P4_32_12$	$P2_1/n$
a (Å)	20.7489(15)	15.8723(10)	14.6671(11)
b (Å)	11.1708(8)	15.8723(10)	23.2288(18)
c (Å)	13.6401(10)	30.180(3)	17.7816(13)
α (°)	90	90	90
β (°)	109.1690(10)	90	103.364(2)
γ (°)	90	90	90
Volume ($Å^3$)	2986.2(4)	7603.2(9)	5894.1(8)
Z	4	8	4
$D_{calcd.}$ (g cm^{-3})	1.809	1.687	1.410
μ (mm^{-1})	2.090	1.668	1.245
F(000)	1572	3784	2548
Crystal size (mm^3)	0.04 × 0.08 × 0.29	0.04 × 0.09 × 0.11	0.07 × 0.15 × 0.20
θ range (°)	2.08 to 28.84	1.45 to 25.00	1.47 to 25.00
Index ranges	$-19 \le h \le 27$	$-18 \le h \le 17$	$-17 \le h \le 15$
	$14 \le k \le 13$	$13 \le k \le 18$	$27 \le k \le 27$
	$18 \le l \le 17$	$35 \le l \le 35$	$21 \le l \le 18$
Collected reflections	9428	40480	30716
Independent reflections	3623 [*R*(int) = 0.0491]	6708 [*R*(int) = 0.3321]	10358 [*R*(int) = 0.1270]
Completeness to θ (%)	92.6 to 28.84	100.0 to 25.00	99.7 to 24.71
Absorption correction	none	none	none
Refinement method	full-matrix least-squares on F^2	full-matrix least-squares on F^2	full-matrix least-squares on F^2
Data/restraints/parameters	3623/0/177	6708/0/447	10358/8/258
Goodness-of-fit on F^2	0.768	0.877	0.993
Final *R* values [$I > 2\sigma(I)$]	*R*1 = 0.0327, *wR*2 = 0.0600	*R*1 = 0.0890, *wR*2 = 0.2112	*R*1 = 0.0908, *wR*2 = 0.2470
R values (all data)	*R*1 = 0.0663, *wR*2 = 0.0716	*R*1 = 0.3155, *wR*2 = 0.3000	*R*1 = 0.2053, *wR*2 = 0.2983
Largest diff. peak/hole (e·$Å^{-3}$)	0.847 and −0.417	1.611 and −1.138	1.925 and −1.092

temperature. MS in $CHCl_3$ (ESI^+): m/z = 808 [$M^+ - I - H_2O$]; (ESI^-): m/z = 1062 [$M^- + I - H_2O$].

Preparation of [$Ru_2Br(\mu\text{-}O_2CCMePh_2)_4(EtOH)$] (5): This complex was prepared by a literature procedure.[19] Single crystals of **5**·0.5EtOH were obtained by the procedure described for complex **1**. MS in DMSO/MeOH (ESI^+): m/z = 1261 [M^+ + DMSO], 1182 [M^+ + DMSO − Br]; (ESI^-): m/z = 1264 [M^- + Br].

Preparation of [$Ru_2I(\mu\text{-}O_2CCMePh_2)_4(MeOH)$] (6): This complex was prepared by a literature procedure.[19] Single crystals of **6**·0.5H_2O were obtained by the following procedure: A solution of [$Ru_2Cl(\mu\text{-}O_2CCMePh_2)_4$] (0.11 g, 0.10 mmol) in MeOH (15 mL), was treated with a water solution of $AgNO_3$ (0.017 g, 0.10 mmol). The solution was filtered and treated with an excess of PPh_4I (0.23 g, 0.50 mmol). Single crystals of **6**·0.5H_2O grew from this solution in 48 h. MS in $CHCl_3$/MeOH (ESI^+): m/z = 1104 [M^+ − I]; (ESI^-): m/z = 1358 [M^- + I].

X-ray Crystallographic Study: Details of the data collection and crystal structure refinement correction for **1**, **2**, **3**·H_2O, **4**·H_2O, **5**·0.5EtOH, and **6**·0.5H_2O are summarised in Table 5 and 6. Suitable crystals were mounted on a Bruker Smart-CCD diffractometer equipped with graphite-monochromated Mo-K_α (λ = 0.71073 Å) radiation. Data were collected at 293(2) K over a quadrant of the reciprocal space by combination of two exposure sets. Each exposure of 20 s covered 0.3 in ω. The cell parameters were refined by least-squares fit of all reflections collected. The structures were solved by Patterson (Ru atoms, SHELXS[33]) and conventional Fourier techniques and refined by full-matrix least-squares on F^2 (SHELXL) (except **6**·0.5H_2O which was refined by full-cycle).[34] Final mixed refinements were undertaken with anisotropic thermal parameters for the nonhydrogen atoms. The hydrogen atoms were included with fixed isotropic contributions at their positions calculated geometrically. Elevated final R values were obtained for **3**·H_2O and **5**·0.5EtOH due to the low quality of these crystals.
CCDC-236884−236889 (for **1**, **2**, **3**·H_2O, **4**·H_2O, **5**·0.5EtOH, and **6**·0.5H_2O, respectively) contain the supplementary crystallographic data for this paper. These data can be obtained free of charge at www.ccdc.cam.ac.uk/conts/retrieving.html [or from the Cambridge Crystallographic Data Centre, 12 Union Road, Cambridge CB2 1EZ, UK; Fax: +44-1223-336033; E-mail: deposit@ccdc.cam.ac.uk].

Acknowledgments

We are grateful to the Ministerio de Ciencia y Tecnología (Dirección General de Investigación, project no. BQU 2000-0643) and the Universidad Complutense de Madrid (project PR3/04-12426) for financial support.

[1] F. A. Cotton, R. A. Walton, *Multiple Bonds Between Metal Atoms*, 2nd edition, Oxford University Press, Oxford, U.K., **1993**.
[2] M. C. Barral, R. Jiménez-Aparicio, J. L. Priego, E. C. Royer, F. A. Urbanos, *An. Quim. Int. Ed.* **1997**, *93*, 277−283.
[3] M. A. S. Aquino, *Coord. Chem. Rev.* **1998**, *170*, 141−202.
[4] [4a] M. W. Cooke, T. S. Cameron, K. N. Robertson, J. C. Swarts, M. A. S. Aquino, *Organometallics* **2002**, *21*, 5962−5971. [4b] C. S. Campos-Fernández, L. M. Thomson, J. R. Galán-Mascarós, X. Ouyang, K. R. Dunbar, *Inorg. Chem.* **2002**, *41*, 1523−1533. [4c] M. Rusjan, B. Donnio, B. Heinrich, F. D. Cukiernik, D. Guillon, *Langmuir* **2002**, *18*, 10116−10121. [4d] H. Miyasaka, R. Clérac, C. S. Campos-Fernández, K. R. Dunbar, *J. Chem. Soc., Dalton Trans.* **2001**, 858−861. [4e] H. Miyasaka, R. Clérac, C. S. Campos-Fernández, K. R. Dunbar, *Inorg. Chem.* **2001**, *40*, 1663−1671. [4f] H. Miyasaka, C. S. Campos-Fernández, R. Clérac, K. R. Dunbar, *Angew. Chem. Int. Ed.* **2000**, *39*, 3831−3835. [4g] Y. Sayama, M. Handa, M. Mikuriya, I. Hiromitsu, K. Kasuga, *Bull. Chem. Soc. Jpn.* **2000**, *73*, 2499−2504. [4h] M. Handa, D. Yoshioka, Y. Sayama, K. Shioni, M. Mikuriya, I. Hiromitsu, K. Kasuga, *Chem. Lett.* **1999**, 1033−1034. [4i] Y. Sayama, M. Handa, M. Mikuriya, I. Hiromitsu, K. Kasuga, *Chem. Lett.* **1999**, 453−454. [4j] M. Handa, Y. Sayama, M. Mikuriya, R. Nukada, I. Hiromitsu, K. Kasuga, *Bull. Chem. Soc. Jpn.* **1998**, *71*, 119−125. [4k] J. L. Wesemann, M. H. Chisholm, *Inorg. Chem.* **1997**, *36*, 3258−3267. [4l] X. Ouyang, C. Campana, K. R. Dunbar, *Inorg. Chem.* **1996**, *35*, 7188−7189.
[5] M. J. Bennett, K. G. Caulton, F. A. Cotton, *Inorg. Chem.* **1969**, *8*, 1−6.
[6] A. Bino, F. A. Cotton, T. R. Felthouse, *Inorg. Chem.* **1979**, *18*, 2599−2604.
[7] T. Togano, M. Mukaida, T. Nomura, *Bull. Chem. Soc. Jpn.* **1980**, *53*, 2085−2086.
[8] D. S. Martin, R. A. Newman, L. M. Vlasnik, *Inorg. Chem.* **1980**, *19*, 3404−3407.
[9] B. K. Das, A. R. Chakravarty, *Polyhedron* **1991**, *10*, 491−494.
[10] M. McCann, A. Carvill, P. Guinan, P. Higgings, J. Campbell, H. Ryan, M. Walsh, G. Ferguson, J. Gallagher, *Polyhedron* **1991**, *10*, 2273−2281.
[11] F. A. Cotton, Y. Kim, T. Ren, *Polyhedron* **1993**, *12*, 607−611.
[12] M. C. Barral, R. Jiménez-Aparicio, J. L. Priego, E. C. Royer, F. A. Urbanos, U. Amador, *Inorg. Chem.* **1998**, *37*, 1413−1416.
[13] F. D. Cukiernik, D. Luneau, J. C. Marchon, P. Maldivi, *Inorg. Chem.* **1998**, *37*, 3698−3704.
[14] M. C. Barral, R. Jiménez-Aparicio, D. Pérez-Quintanilla, E. Pinilla, J. L. Priego, E. C. Royer, F. A. Urbanos, *Polyhedron* **1998**, *18*, 371−376.
[15] M. C. Barral, R. Jiménez-Aparicio, D. Pérez-Quintanilla, J. L. Priego, E. C. Royer, M. R. Torres, F. A. Urbanos, *Inorg. Chem.* **2000**, *39*, 65−70.
[16] M. C. Barral, R. Jiménez-Aparicio, E. C. Royer, C. Ruiz-Valero, M. J. Saucedo, F. A. Urbanos, *Inorg. Chem.* **1994**, *33*, 2692−2694.
[17] M. C. Barral, R. Jiménez-Aparicio, J. L. Priego, E. C. Royer, M. J. Saucedo, F. A. Urbanos, U. Amador, *J. Chem. Soc., Dalton Trans.* **1995**, 2183−2187.
[18] M. C. Barral, R. Jiménez-Aparicio, J. L. Priego, E. C. Royer, F. A. Urbanos, U. Amador, *J. Chem. Soc., Dalton Trans.* **1997**, 863−868.
[19] M. C. Barral, R. González-Prieto, R. Jiménez-Aparicio, J. L. Priego, M. R. Torres, F. A. Urbanos, *Eur. J. Inorg. Chem.* **2003**, 2339−2347.
[20] T. Kimura, T. Sakurai, M. Shima, T. Togano, M. Mukaida, T. Nomura, *Bull. Chem. Soc. Jpn.* **1982**, *55*, 3927−3928.
[21] W. Z. Chen, T. Ren, *Inorg. Chem.* **2003**, *42*, 8847−8852.
[22] W. J. Geary, *Coord. Chem. Rev.* **1971**, *7*, 81−122.
[23] G. J. Norman, G. E. Renzoni, D. A. Case, *J. Am. Chem. Soc.* **1979**, *101*, 5256−5267.
[24] F. A. Cotton, E. Pedersen, *Inorg. Chem.* **1975**, *14*, 388−391.
[25] J. Telser, R. S. Drago, *Inorg. Chem.* **1984**, *23*, 3114−3120.
[26] G. Estiú, F. D. Cukiernik, P. Maldivi, O. Poizat, *Inorg. Chem.* **1999**, *38*, 3030−3039.
[27] R. Jiménez-Aparicio, F. A. Urbanos, J. M. Arrieta, *Inorg. Chem.* **2001**, *40*, 613−619.
[28] C. J. O'Connor, *Prog. Inorg. Chem.* **1982**, *29*, 232 and 244.
[29] [29a] V. M. Miskowski, M. D. Hopkins, J. R. Winkler, H. B. Gray, *Multiple Metal-Metal Bonds*, 343−402, in *Inorganic Electronic Structure and Spectroscopy, Volume II: Applications and Case Studies* (Eds.: E. I. Solomon, A. B. P. Lever), J. Wiley &

Sons, New York, **1999**. [29b] V. M. Miskowski, H. B. Gray, *Inorg. Chem.* **1988**, *27*, 2501−2506. [29c] V. M. Miskowski, T. M. Loehr, H. B. Gray, *Inorg. Chem.* **1987**, *26*, 1098−1108.
[30] [30a] R. J. H. Clark, M. L. Franks, *J. Chem. Soc., Dalton Trans.* **1976**, 1825−1828. [30b] R. J. H. Clark, L. T. H. Ferris, *Inorg. Chem.* **1981**, *20*, 2759−2766.
[31] M. Mukaida, T. Nomura, T. Ishimori, *Bull. Chem. Soc. Jpn.* **1972**, *45*, 2143−2147.
[32] F. A. Urbanos, Program MASAS V 3.1, **2002**.
[33] G. M. Sheldrick, SHELXS-97, Program for the solution of Crystal Structures, University of Göttingen, Germany, **1997**.
[34] G. M. Sheldrick, SHELXL-97, Program for the solution of Crystal Structures, University of Göttingen, Germany, **1997**.

Received May 7, 2004
Early View Article
Published Online October 1, 2004

